# Supplementary Material for: From slab to surface: Earthquake evidence for fluid migration at Uturuncu volcano, Bolivia

Thomas S. Hudson[a,*], J-Michael Kendall[a], Matthew E. Pritchard[b], Jonathan D. Blundy[a], Joachim H. Gottsmann[c]

[a] *Department of Earth Sciences, University of Oxford, UK*
[b] *Department of Earth and Atmospheric Sciences, Cornell University, USA*
[c] *School of Earth Sciences, University of Bristol, UK*

---

This supplementary file contains additional details of some of the methods used in the study described in the main text, as well as Supplementary Figures 1-4 and Supplementary Table 1, referred to in the main text.

## 1. Calculating moment magnitude, $M_w$

In this study, Mw is measured using the spectral method described in Stork et al. (2014). Stork et al. (2014). In order to calculate the moment magnitude, Mw, one first has to measure the seismic moment, $M_0$, of an earthquake, which for a double-couple shear source is defined by,

$$M_0 = \mu D S, \tag{1}$$

where $\mu$ is the shear modulus of the fault, $D$ is the average slip along the fault, and $S$ is the area of the fault over which the slip occurs. $M_0$ can be measured using the long-period displacement spectral amplitude, $\Omega_0$, using the relationship given by Shearer (2009),

$$M_0 = \frac{4\pi\rho v_i^2 r \Omega_0}{A_{rad,i} C_{free-surface}}, \tag{2}$$

⋆
*Corresponding author
*Email address:* thomas.hudson@earth.ox.ac.uk (Thomas S. Hudson)

where $\rho$ is the density of the medium, $v_i$ is the velocity of the seismic phase $i$ (P or S), $r$ is the source-receiver distance, $Arad, i$ is the source radiation pattern correction term for the relevant seismic phase $i$ (again, P or S), and $C_{free-surface}$ is the free surface correction term. $C_{free-surface}$ is given by,

$$C_{free-surface} = 2cos(\theta_i), \tag{3}$$

where $\theta_i$ is the angle of incidence of the plane wave at the surface. The radiation pattern of the earthquakes are not inverted for in this study, and so average values for the radiation pattern for P- and S-waves of $A_{rad,P} = 0.44$ and $A_{rad,S} = 0.6$, respectively, are assumed. Testing of this assumption by others found associated uncertainties of $\pm 0.2 M_w$ for P-waves (Stork et al., 2014). $M_w$ can then be calculated from $M_0$ using the moment magnitude scale proposed by Hanks and Kanamori (1979),

$$M_w = \frac{2}{3} log_{10}(M_0) - 6.0. \tag{4}$$

In order to calculate $M_w$ one therefore needs to estimate the long-period displacement spectral amplitude, $\Omega_0$ from Equation 2. An overview of how $\Omega_0$, and hence $M_w$, are calculated is as follows:

1. The instrument gains and frequency-dependent response are corrected for, to give us the velocity time series in SI units.
2. The velocity signal from each seismometer is integrated over time, in order to obtain the displacement signal associated with an earthquake.
3. The spectrum of the displacement signal is then found. A multi-taper spectrum method (Krischer, 2016; Prieto et al., 2009) is used to compute the spectrum, rather than a single-taper filter, which might introduce bias at particular frequencies.
4. A Brune source model (Brune, 1970) is then fitted to the displacement spectrum to find the long-period displacement spectral amplitude, $\Omega_0$. The Brune model is given by,

$$\Omega(f) = \frac{\Omega_0 e^{-\pi f t^*}}{1 + \left(\frac{f}{f_c}\right)^2}, \tag{5}$$

where $f$ is the frequency, $f_c$ is the corner frequency, and $t^*$ is given by,

$$t^* = \frac{t}{Q}, \tag{6}$$

where $t$ is the travel-time and $Q$ is the quality factor, a measure of the attenuation of the medium. $\Omega_0$, $t^*$, and $f_c$ are varied simultaneously to find the best fitting model source parameters. Examples of this fit are shown in Figure 2 in the main text.

5. $\Omega_0$ and the other relevant parameters are input into Equation 2 to find an estimate of $M_w$ for a particular station.
6. Steps (1) to (4) are then repeated for each station that observed the earthquake. $M_w$ estimates of stations with $Q > 1000$ are not used, since these represent poor Brune source model fits. An overall estimate of $M_w$ for the event is then obtained by taking the mean of all accepted $M_w$ station observations.

## 2. Calculating local magnitude, $M_L$

In order to compare the results of this study with other studies of seismicity at Uturuncu, and other volcanoes more generally, local magnitudes are calculated for the earthquake catalogue. The method of Keir et al. (2006) and Illsley-Kemp et al. (2017) is used to find the $M_L$ values of earthquakes in the catalogue. The process involves:

1. First correcting for the instrument gain and frequency-dependent response, cut the waveforms around the S phase arrival and integrate the velocity data in the time domain to obtain the displacement time series.
2. Find the maximum amplitude on the N and E components.
3. Perform steps (1) and (2) for all earthquakes, until all the observed maximum horizontal amplitudes, $A_{ijk}$, have been measured, where the indices $i$, $j$ and $k$ correspond to the events, stations, and components.
4. Local magnitudes for each event are then calculated using the local magnitude scale, derived by Richter (1935),

$$M_{L,i} = log(A_{ijk}) - log(A_0) + C_{ijk}, \tag{7}$$

where $M_{L,i}$ is the local magnitude for event $i$, $A_0$ is the amplitude reference term, and $C_{jk}$ is the correction term a given station-component pair. Instead of using Richter′s $A_0$, we use the **?** correction, which accounts for the attenuation structure at short epicentral distances. $A_0$ is then defined as,

$$-log(A_0) = n.log\left(\frac{r_{ij}}{17}\right) - K\left(r_{ij} - 17\right) + 2, \tag{8}$$

where $n$ and $K$ are region specific constants to be found. Equation 7 then becomes,

$$M_{L,i} = log(A_{ijk}) + n.log\left(\frac{r_{ij}}{17}\right) - K\left(r_{ij} - 17\right) + 2 + C_{jk}, \tag{9}$$

One can then rewrite this equation in matrix notation (Illsley-Kemp et al., 2017), which takes the form,

$$\begin{pmatrix} log(A_{111})+2 \\ log(A_{112})+2 \\ \vdots \\ log(A_{1N2})+2 \\ log(A_{211})+2 \\ \vdots \\ log(A_{N_eN_s2})+2 \end{pmatrix} = \begin{pmatrix} n \\ K \\ M_{L,1} \\ M_{L,2} \\ \vdots \\ M_{L,N_e} \\ C_{11} \\ C_{12} \\ \vdots \\ C_{N2} \end{pmatrix} \cdot \begin{pmatrix} -log\left(\frac{r_{11}}{17}\right) & -(r_{11}-17) & 1 & 0 & \cdots & 0 & -1 & 0 & \cdots & 0 \\ -log\left(\frac{r_{12}}{17}\right) & -(r_{12}-17) & 1 & 0 & \cdots & 0 & 0 & -1 & \cdots & 0 \\ \vdots & \vdots & \vdots & \vdots & \ddots & \vdots & \vdots & \vdots & \ddots & \vdots \\ -log\left(\frac{r_{1N_s}}{17}\right) & -(r_{1N_s}-17) & 1 & 0 & \cdots & 0 & -1 & 0 & \cdots & -1 \\ -log\left(\frac{r_{21}}{17}\right) & -(r_{21}-17) & 0 & 1 & \cdots & 0 & -1 & 0 & \cdots & 0 \\ \vdots & \vdots & \vdots & \vdots & \ddots & \vdots & \vdots & \vdots & \ddots & \vdots \\ -log\left(\frac{r_{N_eN_s}}{17}\right) & -(r_{N_eN_s}-17) & 0 & 0 & \cdots & 1 & 0 & 0 & \cdots & -1 \end{pmatrix} \tag{10}$$

This equation can then be solved to find $n$, $K$, $M_L$ for every event, and $C_{jk}$ for every station-component pair.

## 3. Calculating overall and temporal variations in b-value

The linear logarithmic relationship described by the Gutenberg-Richter equation (Equation 1, main text) only holds if every earthquake has been detected.

In practice this is only true for part of an earthquake catalogue, i.e. for events with greater magnitudes than the magnitude of completeness, $M_c$. $M_c$ is defined as the magnitude above which the earthquake catalogue is approximately complete. Below the magnitude of completeness, the number of earthquakes detected drops off due to events being below the prevailing noise level, or spatial variation in detection levels due to network coverage, for example. If one has a catalogue of events with assigned magnitudes, then to obtain an estimate of the b-value, it is critical to first calculate $M_c$.

There are various methods for calculating $M_c$, but the method used here is the B-value Stability Criterion (BVS) method (Roberts et al., 2015), which arguably provides a more accurate estimate of $M_c$ than other methods. The method calculates Mc by assessing the stability of b-value with increasing $M_c$. The entire earthquake catalogue is included initially, before being incrementally reduced by increasing $M_c$ until the b-value of this smaller subset of earthquakes remains stable for successive iterations. For each subset, the b-value is defined by (Marzocchi and Sandri, 2003; Shi and Bolt, 1982),

$$b = \frac{1}{ln\,(10)\,(\mu_M - (M_c - \Delta M))}, \tag{11}$$

where $\mu_M$ is the mean magnitude of the subset of earthquakes, $M_c$ is the current artificially set magnitude of completeness, and $\Delta M$ is the width of the magnitude bins used. The standard error associated with the b-value, $\hat{\sigma_b}$, is given by,

$$\hat{\sigma_b} = 2.30b^2\sqrt{\frac{\sum_{i=1}^{N}\left(M_i - \mu_M\right)^2}{N_c\left(N_c - 1\right)}}, \tag{12}$$

where $N_c$ is the number of events in the subset of earthquakes. The b-value is deemed stable when it remains within the uncertainty of a certain number of proceeding earthquake subsets of increasing magnitude of completeness. Here, the number of proceeding subsets required for stability is set to 5. This allows $M_c$ to be estimated in a statistically rigorous manner, which is important given the sensitivity of the b-value to $M_c$.

To assess any variations in stress state, and hence fluid migration, temporal variations in b-value are also calculated. Given that reliable estimates

of b-value are often challenging for entire catalogues, we apply a probabilistic method proposed by Roberts et al. (2016) to obtain the Probability Density Function (PDF) of temporal b-value variation. This has proven successful in other volcanic seismicity studies (Greenfield et al., 2020). The method is as follows:

1. The earthquake catalogue is sorted into chronological order.
2. The chronological earthquake catalogue is then sampled using many different windows of random lengths, back and forth consecutively throughout the time series. The time stamp of the window is assigned as the mean earthquake origin time within the window. We use 5000 windows of uniformly random lengths between 50 and 500 earthquakes.
3. The b-value and associated error are then calculated for each window. These are used to calculate the full b-value PDF of each window, which is assumed to be Gaussian with the mean taking the b-value and the standard deviation taking the b-value error.
4. These individual pdfs for each window are then combined to produce an overall b-value pdf through time. This is done by stacking a certain number of chronological individual window pdfs, 50 in our case. The more individual pdfs that are stacked, the smoother the result in time. The approach of Roberts et al. (2016) is used to determine the optimal stack number, in order to minimise noise in the overall b-value pdf with time, while preserving any real temporal variations.

## 4. Supplementary figures

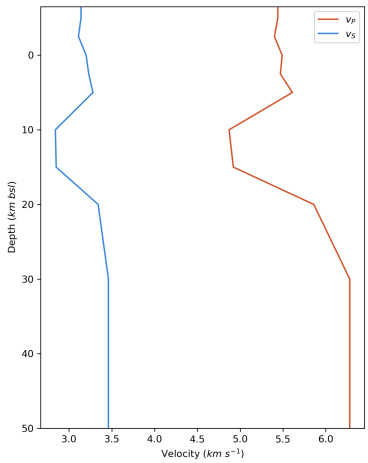


Figure 1: 1D velocity model used in this study. This model is based on the most recent 3D seismic tomography survey available. (Y. Liu, pers. comm.)

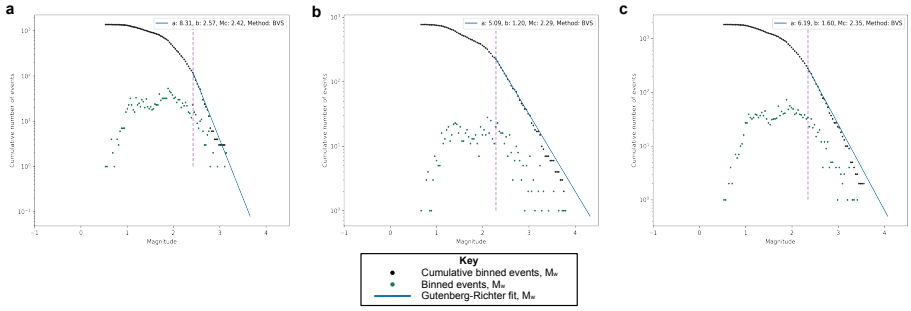


Figure 2: Plots of the cumulative frequency of earthquakes vs. their moment magnitudes for: a) the PLUTONS network only; b) The ANDIVOLC network only; c) The PLUTONS and ANDIVOLC networks combined, but with earthquakes triggered by the 2010 Maule earthquake removed.

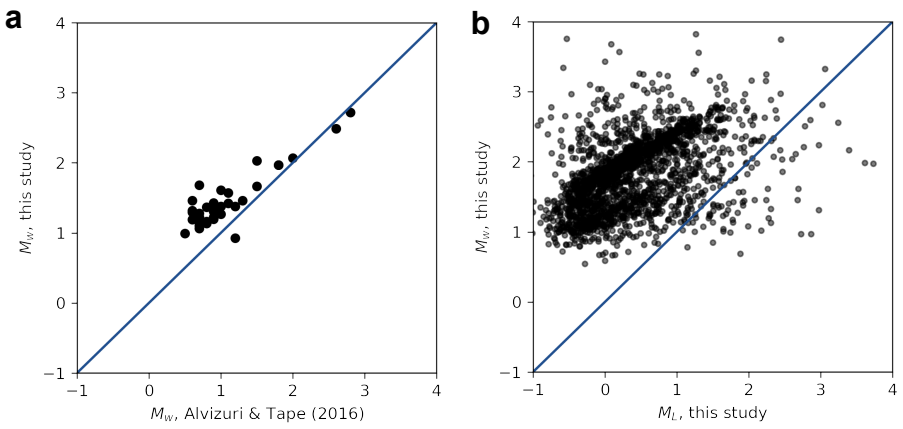


Figure 3: a) Plot of $M_w$ for our results ($M_w$, this study) for earthquakes matched with the $M_w$ values for earthquakes from the full-waveform moment tensor inversion results of Alvizuri and Tape (2016) ($M_w$, Alvizuri and Tape (2016)). The solid line indicates where a 1:1 relationship would lie. b) Same as (a) but comparing $M_w$ from this study with $M_L$ for all the events in this study.

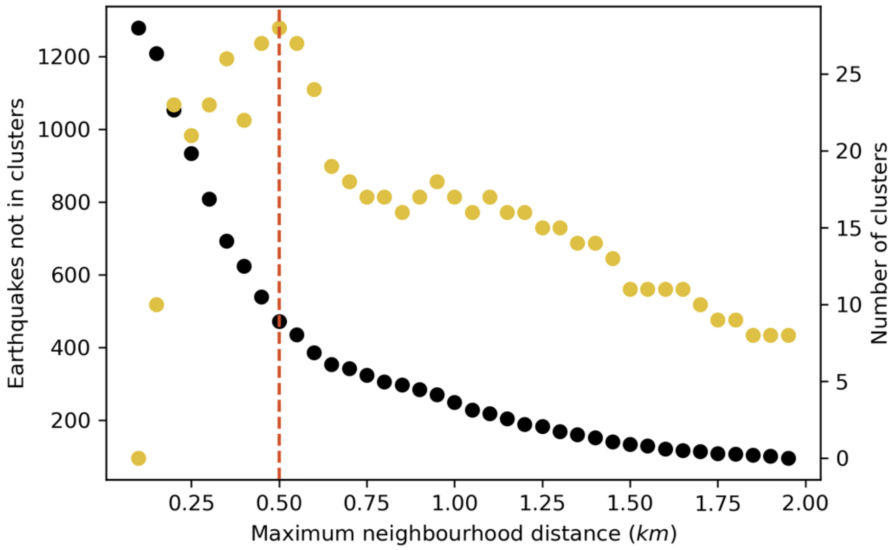


Figure 4: Plot of variation in number of clusters and earthquakes not included in clusters with maximum neighbourhood distance used by the DBSCAN algorithm, for the shallow seismicity data in Figure 5 (main text). The red dashed line indicates the chosen value used for the DBSCAN seismicity clustering analysis presented in Figure 5 (main text).

## 5. Supplementary tables

Table 1: Table of key parameters used by QuakeMigrate and NonLinLoc for detection and location of the earthquake catalogue in this study. We also detail the spatial-temporal uncertainty filters we use to refine the catalogue to remove any false triggers.

| Parameter | Value |
|---|---|
| **QuakeMigrate** | |
| Grid spacing, x, y, z | 0.1 $km$, 0.1 $km$, 0.1 $km$ |
| Detect decimation factors, x, y, z | $6, 6, 4$ |
| Detect sampling rate | 50 $Hz$ |
| P-phase band-pass filter | 2 to 20 $Hz$ |
| P STA/LTA | 0.2 $s$ / 1.0 $s$ |
| S-phase band-pass filter | 2 to 20 Hz |
| S STA/LTA | 0.2 $s$ / 1.0 $s$ |
| Median Absolute Deviation (MAD) multiplier | 8.0 |
| Locate sampling rate (ANDIVOLC, PLUTONS) | 50 $Hz$, 100 $Hz$ |
| **NonLinLoc** | |
| Velocity grid spacing, x, y, z | 0.5 $km$, 0.5 $km$ , 0.5 $km$ |
| LocGau2 velocity model uncertainty settings | 0.05 $s$, 0.02 $s$, 10.0 $s$ |
| **Earthquake catalogue filters** | |
| Maximum depth uncertainty | $\pm$9 $km$ |
| Maximum $t_{rms}$ | 0.6 $s$ |
| Upper depth cut-off | 3 $km$ $asl$ |

## References


Alvizuri, C., Tape, C., 2016. Full moment tensors for small events (Mw<3) at Uturuncu volcano, Bolivia. Geophysical Journal International Advance Access published July 6, 1761–1783. doi:10.1093/gji/ggw247.

Brune, J.N., 1970. Tectonic Stress and the Spectra of Seismic Shear Waves from Earthquakes. Journal of Geophysical Research 75, 4997–5009.

Greenfield, T., White, R.S., Winder, T., Ágústsdóttir, T., 2020. Seismicity of the Askja and Bardarbunga volcanic systems of Iceland, 2009–2015. Journal of Volcanology and Geothermal Research 391. doi:10.1016/j.jvolgeores.2018.08.010.

Hanks, T.C., Kanamori, H., 1979. A moment magnitude scale. Journal of Geophysical Research 84, 2348. URL: http://doi.wiley.com/10.1029/JB084iB05p02348, doi:10.1029/JB084iB05p02348.

Illsley-Kemp, F., Savage, M.K., Keir, D., Hirschberg, H.P., Bull, J.M., Gernon, T.M., Hammond, J.O., Kendall, J.M., Ayele, A., Goitom, B., 2017. Extension and stress during continental breakup: Seismic anisotropy of the crust in Northern Afar. Earth and Planetary Science Letters 477, 41–51. URL: http://dx.doi.org/10.1016/j.epsl.2017.08.014, doi:10.1016/j.epsl.2017.08.014.

Keir, D., Stuart, G.W., Jackson, A., Ayele, A., 2006. Local earthquake magnitude scale and seismicity rate for the Ethiopian rift. Bulletin of the Seismological Society of America 96, 2221–2230. doi:10.1785/0120060051.

Krischer, L., 2016. mtspec Python wrappers 0.3.2. Zenodo doi:10.5281/zenodo.321789.

Marzocchi, W., Sandri, L., 2003. A review and new insights on the estimation of the b-value and its uncertainty. Annals of Geophysics 46, 1271–1282. doi:10.4401/ag-3472.

Prieto, G.A., Parker, R.L., Vernon, F.L., 2009. A Fortran 90 library for multitaper spectrum analysis. Computers and Geosciences 35, 1701–1710. doi:10.1016/j.cageo.2008.06.007.

Richter, C.F., 1935. An instrumental earthquake magnitude scale. Bulletin of the Seismological Society of America 25, 1–32. doi:10.2307/1779766.

Roberts, N.S., Bell, A.F., Main, I.G., 2015. Are volcanic seismic b-values high, and if so when? Journal of Volcanology and Geothermal Research 308,

127–141. URL: http://dx.doi.org/10.1016/j.jvolgeores.2015.10.021, doi:10.1016/j.jvolgeores.2015.10.021.

Roberts, N.S., Bell, A.F., Main, I.G., 2016. Mode switching in volcanic seismicity: El Hierro 2011-2013. Geophysical Research Letters 43, 4288–4296. doi:10.1002/2016GL068809.

Shearer, P.M., 2009. Introduction to Seismology. Second ed., Cambridge University Press.

Shi, Y., Bolt, B.A., 1982. The standard error of the magnitude-frequency b value. The Bulletin of the Seismological Society of America 72, 1677–1687.

Stork, A.L., Verdon, J.P., Kendall, J.M., 2014. The robustness of seismic moment and magnitudes estimated using spectral analysis. Geophysical Prospecting 62, 862–878. doi:10.1111/1365-2478.12134.